The Effect of Myofilament Compliance on Kinetics of Force Generation by Myosin Motors in Muscle

M. Linari, G. Piazzesi, and V. Lombardi*
Laboratorio di Fisiologia, Dipartimento di Biologia Evoluzionistica, Università di Firenze, Sesto Fiorentino, Firenze, Italy

ABSTRACT We use the inhibitor of isometric force of skeletal muscle *N*-benzyl-p-toluene sulfonamide (BTS) to decrease, in a dose dependent way, the number of myosin motors attached to actin during the steady isometric contraction of single fibers from frog skeletal muscle (4°C, 2.1 μm sarcomere length). In this way we can reduce the strain in the myofilament compliance during the isometric tetanus (T_0) from 3.54 nm in the control solution ($T_{0,NR}$) to ~0.5 nm in 1 μM BTS, where T_0 is reduced to ~0.15 $T_{0,NR}$. The quick force recovery after a step release (1–3 nm per half-sarcomere) becomes faster with the increase of BTS concentration and the decrease of T_0. The simulation of quick force recovery with a multistate model of force generation, that adapts Huxley and Simmons model to account for both the high stiffness of the myosin motor (~3 pN/nm) and the myofilament compliance, shows that the increase in the rate of quick force recovery by BTS is explained by the reduced strain in the myofilaments, consequent to the decrease in half-sarcomere force. The model estimates that i), for the same half-sarcomere release the state transition kinetics in the myosin motor are five times faster in the absence of filament compliance than in the control; and ii), the rate of force recovery from zero to T_0 is ~6000/s in the absence of filament compliance.

INTRODUCTION

Muscle contraction is due to an ATP-driven structural working stroke in the head portion of the molecular motor myosin II, while it is attached to the actin filament. In situ the myosin motors work in parallel in each half-sarcomere and this makes necessary to study myosin function in the assembled system, like in a muscle fiber. In this case, however, the study is complicated by the fact that each half-sarcomere is in series with thousands of other half-sarcomeres and the fiber is connected to the transducers via the compliant tendon attachments. A further complication is represented by the finding that a large proportion of the compliance of the half-sarcomere (>50%) is in the actin and myosin filaments (1–4). The large myofilament compliance limits the possibility to define the number and the kinetics of myosin motors working in each half-sarcomere by means of length step perturbation experiments (5). In fact, because of the presence of constant myofilament compliance, the change in the elastic response of the half-sarcomere underestimates the actual change in the number of myosin motors. Moreover, the quick force recovery after a step release, that represents the mechanical manifestation of the working stroke in the myosin motors (5), is slowed by myofilament compliance, because the drop in motor strain induced by the release is much less than that expected from the size of release and the motors move during force recovery to reload the filament compliance. Consequently, the rate of quick force recovery underestimates the kinetics of transition among different force generating states in the myosin motor (6).

Recent applications of sarcomere-level mechanical methods to single fibers from vertebrate skeletal muscle (7–9) made it possible to analyze the contributions of myofilaments and myosin motors to the half-sarcomere compliance and define the number and the force of the motors during the isometric contraction and their distortion after stepwise changes in length or force. No direct measurement has been reported so far on the effects of the filament compliance on the kinetics of quick force recovery after a step in length of the half-sarcomere, neither the kinetics of state transitions in the myosin motor free from the myofilament compliance have been evaluated.

It has been reported that *N*-benzyl-p-toluene sulfonamide (BTS), in the micromolar range, suppresses twitch and tetanic force of fast vertebrate skeletal muscle by binding to subfragment 1 (S1) of the myosin head, without affecting Ca^{2+} regulation (10,11). Solution kinetic studies show that inhibition by BTS of the myosin-actin ATPase cycle is accompanied by the reduction of the rate of Pi release (12). In this work, using half-sarcomere stiffness measurements in single frog fibers at 4°C and 2.1 μm sarcomere length, we show that BTS decreases, in a dose dependent way, the isometric tetanic force (T_0) and the number of attached myosin motors, down to ~15% of the control values with [BTS] 1 μM, without affecting the force per motor. Under these conditions, although the strain in the myosin motor remains constant, the contribution to the half-sarcomere compliance of the equivalent myofilament compliance (the strain in the myofilaments for a change in force equal to T_0) decreases in proportion to the BTS-induced decrease in T_0. The quick force recovery after a step release (1–3 nm per half-sarcomere) becomes faster with the increase of BTS concentration and the decrease of T_0. Simulation of the quick force recovery with a multistate model of force generation, that adapts

Submitted July 15, 2008, and accepted for publication September 29, 2008.
*Correspondence: vincenzo.lombardi@unifi.it
Editor: Hideo Higuchi.

0006-3495/09/01/0583/10 $2.00
doi: 10.1016/j.bpj.2008.09.026

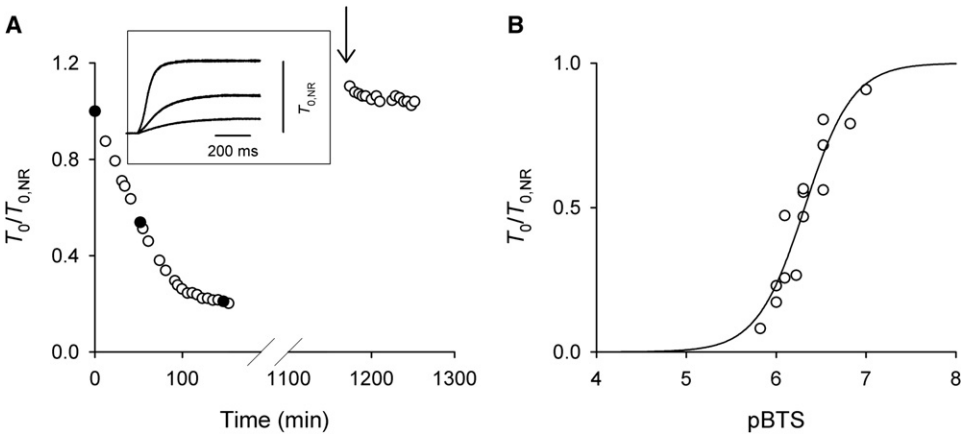

FIGURE 1 Effect of BTS on the isometric force. (*A*) Time course of decay of isometric tetanic force (T_0) after the addition of 1 μM BTS to normal Ringer solution. After ~2 h, T_0 attains a steady value ~0.15 the isometric force in the control solution ($T_{0,NR}$); 8 h before the time indicated by the arrow, the fiber was transferred in normal Ringer solution. Isometric force completely recovers to the initial value. Values are relative to $T_{0,NR}$. Inset: isometric tetani developed in NR and 52 and 147 min after the addition of 1 μM BTS. The three tetanic forces are reported (*solid circles*) on the T_0 - time plot. Fiber length, 6.04 mm; CSA, 13,200 μm^2; average sarcomere length, 2.06 μm; temperature, 4.2°C. (*B*) Dependence of the isometric force, relative to the control value ($T_{0,NR}$), on BTS concentration (expressed in negative log units). $T_{0,NR}$, 300 ± 25 kPa (mean ± SE, 10 fibers). The solid line is the Hill equation (1/(1+10^(n × (pK-pBTS))) fitted to the experimental data. The parameters of the fit are: n, 1.63 ± 0.26 and pK, 6.32 ± 0.03.

the Huxley and Simmons (5) model to account for the high stiffness of the myosin motor (~3 pN/nm (7,9)), shows that for a given step release the increase in the rate of quick force recovery by BTS is accounted for by the reduced effects of filament compliance consequent to the reduced half-sarcomere force and strain.

METHODS

Fiber preparation and apparatus

Frogs (*Rana temporaria*) were killed by decapitation, followed by destruction of the spinal cord, following the official regulation of the European Community Council, Directive 86/609/EEC. Single fibers (5–6 mm long) were dissected from the lateral head of the tibialis anterior muscle and mounted in a thermoregulated aluminum trough between the levers of a fast capacitance force transducer (resonant frequency 30–50 kHz (13)), and a servocontrolled loudspeaker motor (14)). The length change of a population of sarcomeres in a selected fiber segment (0.7–2.0 mm long) was monitored by a striation follower with a time constant of 2 μs and a sensitivity of 125 mV/nm per half-sarcomere (15). The temperature of the bath was set to 4°C. Further details on the experimental apparatus have already been reported ((14) and references therein).

Experimental protocol

The sarcomere length, width and height of the fiber were measured at 0.5 mm intervals along the fiber with a 40× dry objective (NA 0.60, Zeiss, Oberkochen, Germany) and 8× or 25× eyepieces. The cross-sectional area (CSA) was determined assuming the fiber cross section as elliptical. Sarcomere length was set to ~2.1 μm. The fiber was tetanically stimulated with trains of alternate polarity pulses (0.5 ms duration) at a frequency (20–25 Hz) optimal for fused tetanus at 4°C. Time interval between tetani (0.4–0.5 s duration) was 4 min. After the force had attained the tetanic plateau, step changes in length (complete in 110 μs, maximum range −15–+3 nm per half-sarcomere, negative sign for releases) were applied. The length control system was switched from fixed-end to sarcomere length clamp 30 ms before the step and switched back to fixed-end mode at the time of the last stimulus. For step releases larger than that necessary for the fiber to become just slack during the phase 1 response, the duration of the step was increased according to the increase in its amplitude or by recording the force transient in the fixed-end mode. The force attained at the end of the quick force recovery (T_2) was estimated according to the tangent method already described (16,17).

Stiffness was calculated from the slope of the relation between T_1 (the extreme force attained during the length step) and the step amplitude (T_1 relation) for steps in the range −3–+3 nm per half-sarcomere. Temperature was then raised to room temperature (18–20°C) and the normal Ringer (NR) solution was substituted with Ringer solution containing BTS. The effect of BTS on isometric force takes ~2 h to be complete (Fig. 1 *A*), without substantial effect of temperature (between room temperature and 4°C). The time course of the effect was monitored by recording isometric tetani at 10–20 min intervals. Temperature was set to 4°C and the same protocol for stiffness measurements as in the control solution was repeated. The fiber was stimulated tetanically at the same frequency as in the control. The recovery from the effect of BTS takes hours even at room temperature. Therefore, at the end of the experiment, the fiber was dismounted and stored overnight in the refrigerator (~4°C) in NR solution. The day after (7–9 h from the end of the experiment) the fiber was mounted again in the experimental set-up and control measurements were done. Only in three out of the 10 fibers used in these experiments, were three different concentrations of BTS tested. The relation between the level of force attained at the end of quick recovery (T_2) and the step size (T_2 relation (5)) was determined in three fibers in control and in 0.60 ± 0.17 μM BTS.

Solutions

Ringer solution had the following composition (mM): 115 NaCl, 2.5 KCl, 1.8 $CaCl_2$, 3 phosphate buffer (2.15 Na_2HPO_4 and 0.85 NaH_2PO_4) at pH 7.1. BTS (Sigma-Aldrich, catalog No. S949760, or kindly supplied by Chemper, Comeana Carmignano, Prato, Italy), dissolved in dimetyl sulfoxide (stock solution, 10 mM concentration), was added to the Ringer solution in micromolar range (0.1–1.5 μM).

Data recording and analysis

Force, motor position and sarcomere length signals were recorded with a multifunction I/O board (PCI-6110E, National Instruments, Austin, TX) and a dedicated program written in LabVIEW (National Instruments) was used for signal recording and analysis. Force and motor position were also monitored on a chart recorder (Multitrace 2 Recorders 5022, Lectromed, Letchworth Garden City, UK) at a speed of 10 mm/s. Unless otherwise specified, values are expressed as mean ± SE.

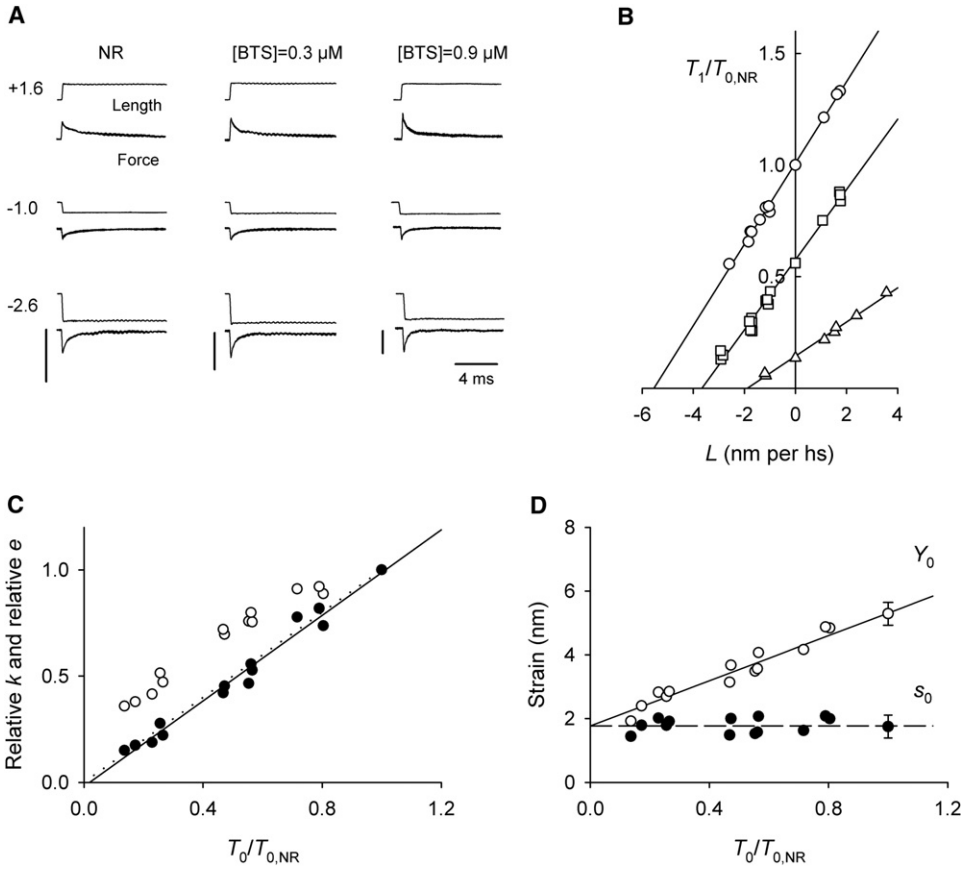

FIGURE 2 Effect of BTS on the stiffness of the half-sarcomere (*A*) Force response (*lower traces*) to different step changes in half-sarcomere length (*upper traces*). Step size is indicated by the figures on the left of each row, in control (*NR*, *left column*) and in the presence of 0.3 μM BTS (*central column*) and 0.9 μM BTS (*right column*). Calibration bars indicate the isometric force in the control (325 kPa), and in BTS (0.3 μM, 180 kPa and 0.9 μM, 50 kPa). Fiber length, 5.74 mm; length of the fiber segment under sarcomere length control, 1.27 mm; sarcomere length, 2.11 μm; CSA, 8,400 μm^2; temperature, 4.4°C. (*B*) Relation between T_1 and the amplitude of the step (L) in the control (*circles*) and in the presence of 0.3 μM BTS (*squares*) and of 0.9 μM BTS (*triangles*). T_1, normalized for the isometric force in control ($T_{0,NR}$). The solid lines are the linear regressions to each set of points in the range −3–+3 nm per half-sarcomere. The slopes (an estimate of the half-sarcomere stiffness) are 0.182 ± 0.003 nm^{-1} in normal Ringer, 0.157 ± 0.004 nm^{-1} in 0.3 μM BTS and 0.077 ± 0.003 nm^{-1} in 0.9 μM BTS. The same fiber was used as in *A*. (*C*) Half-sarcomere stiffness (k, *open circles*) versus isometric force in the range of BTS concentrations used. Both the isometric force and k are relative to their respective control values. Solid circles are the fraction of attached myosin heads (e) relative to the fraction in control conditions, as explained in the Results section. The dotted line is the identity line. The solid line is the linear regression fitted to the data. The slope and the ordinate intercept of the line are 1.01 ± 0.04 and -0.02 ± 0.03, respectively. (*D*) Relation of half-sarcomere strain (Y_0, *open circles*) and motor strain (s_0, *solid circles*) against isometric force at different BTS concentrations. Force is relative to the value in normal Ringer solution. The solid line is the linear regression equation ($Y_0 = s_0 + C_f \times T_0/T_{0,NR}$) fitted to the open circles (slope (C_f) and ordinate intercept (s_0) 3.54 ± 0.19 nm/$T_{0,NR}$ and 1.77 ± 0.15 nm, respectively) and the dashed line is the linear regression to the solid circles (slope and ordinate intercept 0.001 ± 0.194 nm/$T_{0,NR}$ and 1.77 ± 0.15 nm, respectively).

RESULTS

Effect of BTS on the isometric force and stiffness of the half-sarcomere

Fig. 1 *A* shows the time course of the effect of 1 μM BTS on the isometric tetanic force (T_0), as well as its recovery in control solution (NR solution). The relation between BTS concentration (expressed in negative log units, pBTS) and steady isometric force is shown in Fig. 1 *B*. 50% depression of T_0 was attained with ~0.6 μM BTS and 80–90% depression with 1.5 μM. Fitting the Hill equation $(T_0/T_{0,NR}) = \left(1/1 + 10^{n\times(pK-pBTS)}\right)$ to the experimental points shows that n (the order of the reaction) is close to 2, that is two molecules of BTS are necessary for the motor inhibition. In the four fibers where the recovery process was tested, after 8 h from the restoration of NR solution at 4°C, T_0 had recovered 0.95 ± 0.12 (mean ± SD) of the original value.

Fig. 2 *A* shows the force responses to length steps of three different sizes (+1.6, −1.0, and −2.6 nm per half-sarcomere, hs) superimposed on the isometric tetani in the control solution (*left column*) and in solution with 0.3 μM BTS (*central column*) and 0.9 μM BTS (*right column*). The extreme force attained at the end of the step (T_1 (5)) is plotted as a function of the step amplitude L (T_1 relation) in Fig. 2 *B* for the control solution (*circles*) and for the solutions with 0.3 μM BTS (*squares*) and 0.9 μM BTS (*triangles*). The stiffness of the half-sarcomere (k) is measured by the slope of the straight line fitted to the T_1 points in the range of steps −3–+3 nm per hs. Pooled data from 10 fibers show that k decreases with the increase of BTS concentration, but the decrease is less than proportionate to the isometric force (Fig. 2 *C*, *open circles*). The abscissa intercept of the T_1 relation, Y_0, that measures the strain in the elastic components of the half-sarcomere during the isometric contraction preceding the step (16), decreases linearly with the BTS dependent decrease in T_0 (Fig. 2 *D*, *open circles*). The solid line in Fig. 2 *D* is the linear regression equation fitted to Y_0–T_0 points for the range of BTS concentrations used (0–1.5 μM). The slope and the ordinate intercept of the line are 3.54 ± 0.19 nm T_0^{-1} and

1.77 ± 0.15 nm respectively. It is evident, from the overall linear elasticity of the half-sarcomere, that its components (attached myosin motors and actin and myosin filaments) also have linear characteristics. The following analysis provides the mechanical parameters of these components. In these fibers the isometric force in the control solution ($T_{0,NR}$) is 300 ± 25 kPa, consequently the slope of the relation Y_0-T_0 estimated by the fit becomes 0.012 ± 0.001 nm kPa^{-1}, a value fully accounted for by the equivalent compliances of the actin and myosin filaments (C_f) estimated from mechanical and x-ray structural experiments (9,18,19). The ordinate intercept, then, is the average strain in the motors attached to actin in the isometric contraction (s_0 (8,9,18,19)). s_0 at any isometric force (*solid circles* in Fig. 2 *D*) is calculated by subtracting the filament strain ($C_f \times T_0/T_{0,NR}$) from the half-sarcomere strain Y_0. s_0 maintains the same value as in the control in the whole range of the isometric forces. From this analysis it derives that the contribution of myofilaments to the half-sarcomere strain decreases in proportion to the reduction of T_0: in control solution the relative contribution is (3.54/5.4 =) 0.66 and decreases to (1.77/3.7 =) 0.48 at 0.5 $T_{0,NR}$ (0.6 μM BTS) and to (0.5/2.3 =) 0.21 at 0.14 $T_{0,NR}$ (1 μM BTS). The stiffness of the array of motors attached in the half-sarcomere at any BTS concentration is given by T_0/s_0 (*solid circles* in Fig. 2 *C*). The solid line in Fig. 2 *C* is the linear regression equation fitted to solid circles and indicates that, under the assumption that the stiffness of the individual motors is constant at any BTS concentration, the fraction of attached motors decreases in proportion to the BTS-induced decrease in the force of the half-sarcomere. Thus the depressant effect of BTS is exerted only on the number of motors, without any effect on the average force exerted by individual motors. Note that the kinetics of motor detachment, as estimated by the force-velocity relation, is not affected by BTS (see the Supplementary Material).

Effect of BTS on the quick force recovery after a length step

It is evident from direct inspection of the force traces in Fig. 2 *A* that in the presence of BTS the rate of quick force recovery (r) is faster than in the control and that the effect is larger at larger BTS concentration. In Fig. 3 *A*, r, measured by the reciprocal of the time taken for the force to recover from T_1 to $T_1 + 0.63 \times (T_2 - T_1)$, is plotted versus the step amplitude (L) for the control solution (*circles*) and for the solutions with 0.3 μM BTS (*squares*) and 0.9 μM BTS (*triangles*). The analysis is limited to step releases <4 nm to avoid slack in the fiber. In all conditions the rate of recovery is faster going from the stretch to the larger release (5). With the increase in BTS concentration, $r - L$ relations are progressively shifted upward. The dependence of r on BTS-modulated isometric force is shown in Fig. 3 *B* (*open circles*) for the 1.83 ± 0.05 nm release (three experiments). It can be seen that, for decreases in isometric force to ~0.5 $T_{0,NR}$ and ~0.2 $T_{0,NR}$, r increases by 2 and 3 times respectively.

The relations between the force attained at the end of quick recovery (T_2 (5)) and the step amplitude (T_2 relation) both in control solution (*circles*) and in 0.60 ± 0.17 μM BTS (that reduced T_0 to ~0.5 $T_{0,NR}$, *triangles*) are shown in Fig. 3 *C*. Like the control also the BTS T_2 relation shows a downward concavity in the region of small releases (5) and, for releases >6 nm per hs, a linear drop proportional to the step size. Dashed lines are the first order regression equations fitted to the linear part of T_2 curves (see also Piazzesi et al. (17)). It can be seen that the slope of the relation in 0.6 μM BTS is smaller (0.058 nm^{-1}) than that in the control solution (0.104 nm^{-1}). Moreover, the intercept of the regression lines on the length axis L_0 (that represents the maximum sliding distance accounted for by phase 2 process) is smaller in 0.6 μM BTS (13.1 ± 0.1 nm) than in the control solution (14.4 ± 0.6 nm). L_0 is the sum of the discharge of the half-sarcomere strain present in the isometric contraction (Y_0, Fig. 2 *B*) and of the myosin working stroke elicited by shortening (L_s). Thus $L_s = L_0 - Y_0$. According to recent mechanical and x-ray structural evidences (18,20), the axial movement of the myosin motors with respect to the position at T_0 (Δz, where z is the axial position of the motor defined as the distance between the head-rod junction and the point of attachment of the catalytic domain on the actin filament (21)) attains its maximum value L_s when the working stroke is executed under unloaded conditions. In general, for any size of release or for any force T_i during phase 2, Δz can be calculated from the difference between the amount of half-sarcomere shortening (L) and the change in filament strain with respect to the isometric strain

$$\Delta z = L - C_f \times (T_i - T_0), \quad (1)$$

where $C_f \times (T_i - T_0)$ is the change in filament strain (Δs_f).

When the T_2/T_0 points are plotted versus Δz (Fig. 3 *D*), the relation in 0.6 μM BTS (*triangles*) coincides with that in control solution (*circles*). This demonstrates that not only the isometric force but also the size of the working stroke of the myosin motor is unaffected by BTS.

DISCUSSION

BTS reduces the number of motors attached to actin without effect on their function

In this work we demonstrate that BTS in the range of concentrations up to 1.5 μM decreases the isometric force down to 15% of the control value in a dose dependent manner and in a reversible way (see Fig. 1). The force decrease is accompanied by the progressive reduction of the half-sarcomere strain (see Fig. 2 *D*). The slope of the linear fit to the strain-force relation corresponds to the equivalent compliance of the actin and myosin filaments (0.012 nm/kPa) determined in previous x-ray and mechanical studies (1–3,9,18,19). Consequently, the strain in the myosin motors (s) responsible for

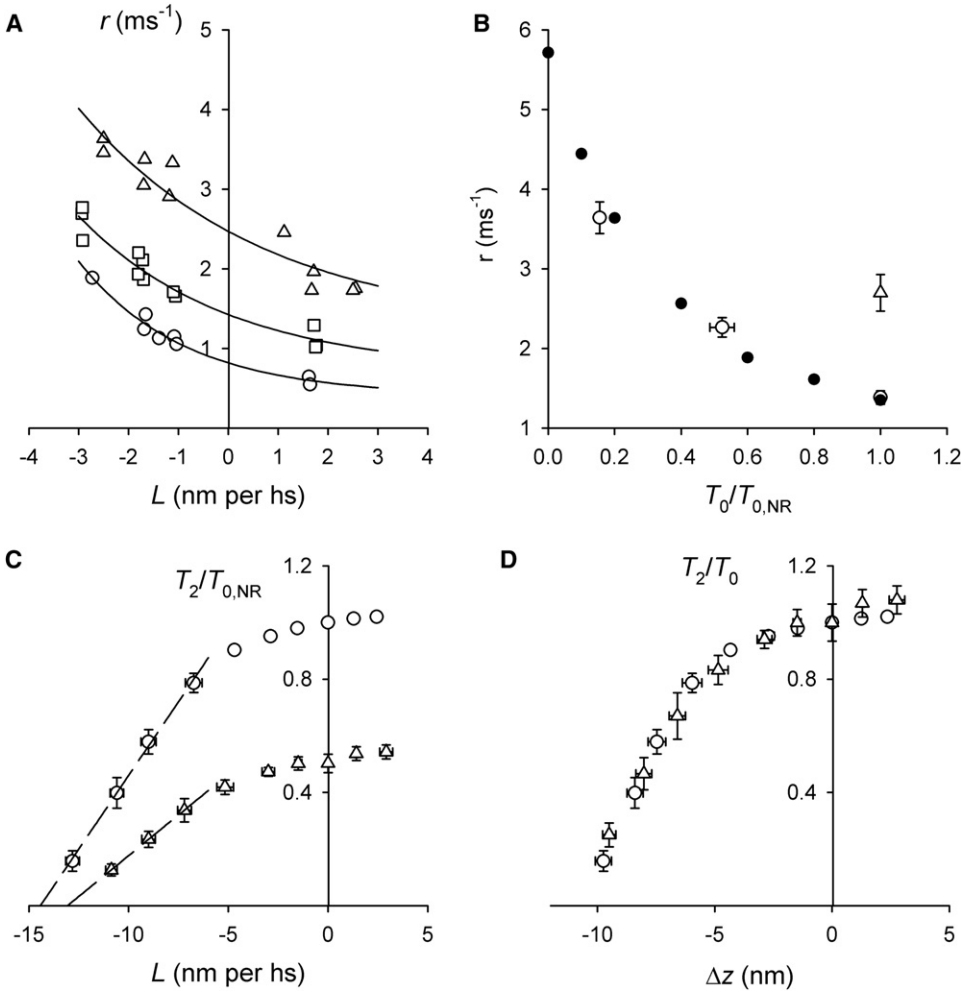

FIGURE 3 Effect of BTS on the quick force recovery. (*A*) Rate constants of quick force recovery (r) after length steps of different amplitudes (L) in either control solution (NR) or in the presence of BTS (0.3 μM, *squares*; 0.9 μM, *triangles*). The lines fitted to the data are obtained by using the exponential equation $r = r_0/2 \times (1+\exp(-\alpha \times L))$ from Huxley and Simmons (5), where L is the amplitude of the step, r_0 is the ordinate intercept of r and α is a constant with dimension nm^{-1}. r_0 and α are the free parameters. Values of r_0 (ms^{-1}) and α (nm^{-1}) are respectively 0.82 ± 0.04 and 0.47 ± 0.03 in the control solution, 1.43 ± 0.06 and 0.34 ± 0.03 in 0.3 μM BTS and 2.47 ± 0.08 and 0.27 ± 0.03 in 0.9 μM BTS. The same fiber was used as described in Fig. 2 *A*. (*B*) Open circles show the effect on r of the BTS modulated isometric force for a step release of 1.83 ± 0.05 nm (mean ± SE, data pooled from three fibers). The two BTS concentrations are 0.56 ± 0.03 μM (0.52 $T_{0,NR}$) and 0.95 ± 0.05 μM (0.16$T_{0,NR}$). The open triangle is r for a step release sufficient to drop the isometric force to zero in the control. Solid circles indicate the simulated rate of force recovery for a step release of 1.85 nm, with different contributions of myofilament compliance to half-sarcomere compliance, as explained in the Results section. (*C*) Relation between T_2, normalized for the isometric force of the control ($T_{0,NR}$), and L in the control solution (*circles*) and in the presence of 0.60 ± 0.17 μM BTS (*triangles*). Mean values (± SE) from three fibers. (*D*) Relation of T_2 (normalized for the isometric force (T_0) preceding the step) versus axial motion of the myosin motors (Δz), obtained by subtracting the strain in the myofilament (Δs_f) from the step length change (L).

the isomeric force is the same at any BTS concentration as in the control (1.8 nm) and the decrease in the isometric force is explained solely by a proportional decrease in the number of force-generating motors working in parallel in each half-sarcomere (see Fig. 2 *C*). This conclusion is supported by the recent crystallographic evidence that another force inhibitor of myosin II, blebbistatin (22), quite similar to BTS in its structure and in the action on actomyosin kinetics (23), binds in the 50 kDa cleft of the motor domain (24), preventing in this way the cleft closure on actin and the formation of a strong actomyosin bond.

The maximum size of the working stroke, as estimated by the abscissa intercept of the T_2 curve, appears to decrease with BTS (Fig. 3 *C*). However, when the decreased filament strain in the BTS isometric contraction is taken into account (by subtracting the change in filament strain from the imposed half-sarcomere shortening), the size of the working stroke is the same in BTS as in the control (Fig. 3 *D*).

BTS as a tool to modulate the amount of equivalent filament compliance in the half-sarcomere

BTS does not affect the function of the myosin motor during its interaction with the actin filament, but only reduces, in a dose dependent manner, the formation of the strong force-generating acto-myosin bond. On the other hand, the decrease in strain of myofilaments with BTS-induced decrease in isometric force acts as if the equivalent compliance in series to the array of motors working in parallel in the half-sarcomere were decreased. In the control solution the myofilament equivalent compliance is (3.54/5.4) ~2/3 of the half-sarcomere compliance and thus twice the motor compliance, whereas in 0.9 μM BTS, when the isometric force is decreased to ~0.14 $T_{0,NR}$, the contribution of myofilaments to the half-sarcomere compliance is (0.5/2.3) ~1/5 (see Fig. 2 *D*). This does not affect either the motor force or the working stroke elicited during the plateau of an isometric contraction,

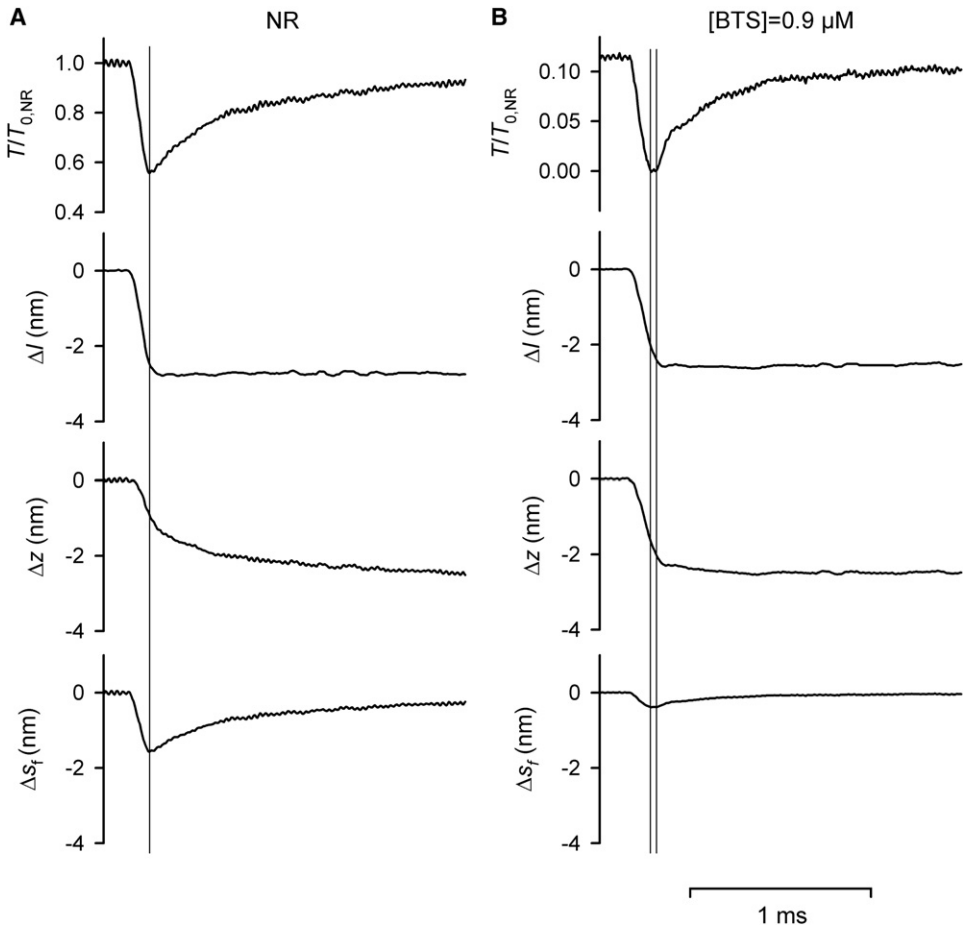

FIGURE 4 Modulation of equivalent myofilament compliance by BTS. Mechanical responses to a step release of ~2.6 nm imposed during isometric contraction in control solution (*A*) and in 0.9 μM BTS (*B*). In each column, from the top to the bottom: time course of force (T) relative to isometric force in the control ($T_{0,NR}$), length change of the half-sarcomere (Δl), axial motion of myosin motors (Δz) and change in the strain of the myofilaments (Δs_f). Vertical line in *A* and leftward vertical line in *B* mark the time for T_1 (that attains zero force in *B*); rightward vertical line in *B* marks the time when the force starts to redevelop from zero. In between the two lines the change in length is only due to motor motion because force stays constant at zero.

because, due to detachment/attachment of motors, the different degree of strain in the myofilaments does not bias the steady-state equilibrium distribution between different force generating states of the motor.

However, during the phase 2 response after a length step, when motors attached to actin react to the decreased stress and recover force by synchronized state transitions, the rate of force rise is expected to be influenced by the filament compliance. An increase in BTS, that decreases the absolute isometric force, decreases also the strain in the filaments. In this way the fraction of the step release that is taken by the motors increases and the movements of motors to reload the filaments in phase 2 decreases. This is made evident in Fig. 4, where the changes in filament strain and the motor movement (Δz) after a step release of 2.6 nm per half-sarcomere are calculated using (Eq. 1) and the force transient of Fig. 2 *A*. In the control solution (Fig. 4 *A*): i), in phase 1, with a force drop to $T_1 = 0.55\ T_{0,NR}$, 2/3 of the step release imposed on the half-sarcomere are taken by myofilaments and only 1/3 is taken by the attached motors, producing an average Δz of ~1 nm; and ii), during phase 2 recovery to $0.93\ T_{0,NR}$, when force is generated by the motor working stroke at constant sarcomere length, Δz increases up to 2.6 nm, with an additional working stroke (1.6 nm) that is almost three times larger than that necessary to strain the motor elasticity ($s_0 \times (T_2 - T_1)/T_{0,NR} = 0.67$ nm). In 0.9 μM BTS ($T_0 = 0.12\ T_{0,NR}$, Fig. 4 *B*): i), in phase 1, only ~20% of the 2.2 nm release necessary to drop force to zero is taken by the myofilaments and 80% by the motors, producing a Δz of ~1.8 nm; ii), after the 30 μs of slack due to the continuation of the release up to 2.6 nm, during which the myosin motors move by further 0.4 nm without change in filament extension, the phase 2 recovery to $0.1\ T_{0,NR}$ at constant sarcomere length implies a further motor movement of 0.35 nm, corresponding to the working stroke necessary to re-strain the myofilaments ($C_f \times 0.1\ T_{0,NR} = 3.54 \times 0.1$), that this time is only ~20% of the working stroke necessary to reload the motor elasticity ($s_0 \times (T_2 - T_1)/T_0 = 1.5$ nm).

The model simulation in the next section is applied to test whether the decrease of the equivalent compliance of myofilaments accompanying isometric force depression by BTS can per se explain the increase of the rate of the quick force recovery after a step release (see Fig. 3 *A* and *B*).

The kinetics of force generation in the motor and the effect of myofilament compliance

Huxley and Simmons (5) theory for force generation predicts that the relation between the rate of the quick force recovery

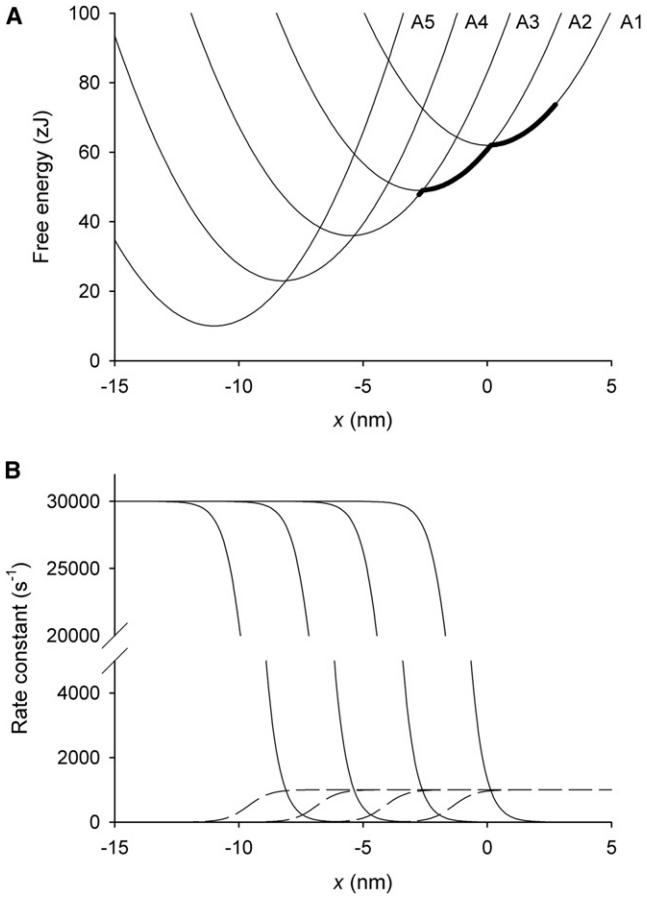

FIGURE 5 Relevant parameters of the mechanical-kinetic model for force generation in the attached motor. (*A*) Free energy diagrams of the myosin motor states (*A1–A5*) as a function of the relative position (*x*) between the myosin head and the actin monomer. *x* is set to zero in correspondence of the minimum free energy of an attached motor in state *A1*. Axial distribution of motors during the isometric contraction (range −2.75–+2.75 nm) marked by the thick line. (*B*) Functions expressing the *x*-dependence of the rate constants for the forward (*solid lines*) and the backward (*dashed lines*) transitions.

after a step in sarcomere length and the size of the step can be used to estimate the strain dependence of the rate constants for transitions between different force generating states of the myosin motor. This has been considered valid because, at the time the theory was formulated, the compliance of the half-sarcomere was almost fully attributed to the compliance in the myosin motors themselves. Under those conditions the state transitions responsible for the quick force recovery would occur at the motor position defined by the amplitude of the step, so that the rate of recovery would be defined only by the strain dependence of the transition rates.

The finding that in fibers of skeletal muscle of *R. temporaria* 65% of the half-sarcomere compliance is functionally in series to the myosin motors has several related consequences: i), during the elastic response the reduction in motor distortion is only 35% of the half-sarcomere shortening imposed with the step release; ii), the rate of quick force recovery after the release is slowed by the motor motion in the shortening direction to reload the filament compliance and cannot be used as a direct estimate of state transition kinetics; and iii), during the force recovery the values of the rate constants controlling the state transitions change according to their dependence on the relative position of the myosin motor and the actin filament. Accordingly, the rate of quick force recovery is reduced with respect to that expected for a given step in the absence of filament compliance and, if the equivalent myofilament compliance is decreased as with BTS-induced depression of isometric force, the rate of phase 2 recovery increases providing a closer estimate of the rate constants of state transition.

To test this idea, the force transient after a step release is simulated with a modified version of the kinetic-mechanical model of the myosin motor (25), that integrates Huxley and Simmons theory of force generation with the presence of filament compliance (see Appendix). The first step in the simulation is to select the rate equations of state transitions that best fit the time course of the quick force recovery after the step release of 1.85 nm per half-sarcomere in control solution ($r = 1380 \pm 80\ s^{-1}$, *rightmost open circle* in Fig. 3 *B*).

The rate of quick force recovery is estimated from the simulated response with the same method used for the experimental records and plotted in Fig. 3 *B* (*rightmost solid circle*). Then the chosen set of rate equations is applied without any modification to the simulation of quick force recovery for the cases in which the myofilament compliance in series to the motors is progressively decreased in steps of 20% of the compliance in the control down to zero. The values of *r* measured from the simulated responses (see *solid circles* in Fig. 3 *B*) interpolate the experimental values (*open circles*, obtained with BTS 0.56 ± 0.03 μM and 0.95 ± 0.05 μM) quite satisfactorily indicating that the increase in *r* by BTS is fully explained by the reduced contribution of myofilaments to half-sarcomere compliance. The simulation predicts that the rate of quick force recovery in the absence of filament compliance is 5700 s^{-1}, five times higher than that estimated in control solution. Note that in the absence of filament compliance the 1.8 nm release is just right to drop the isometric force to zero. Thus 5700/s is the value of *r* when the motor recovers from zero force. In the control this condition occurs with releases of 4-5 nm, due to the large proportion of release taken by filament compliance. The corresponding value of *r*, measured in previous experiments (17,26,27) for a step release of 4.85 ± 0.25 nm, is 2700 ± 400 s^{-1} (see *triangle* in Fig. 3 *B*), ~50% smaller, due to the motor motion against filament compliance during force recovery.

APPENDIX: MODEL SIMULATION OF THE QUICK FORCE RECOVERY

The simulation is based on an earlier version of the kinetic-mechanical model of the myosin motor (25), and integrates Huxley and Simmons theory of force generation with the presence of filament compliance. The model

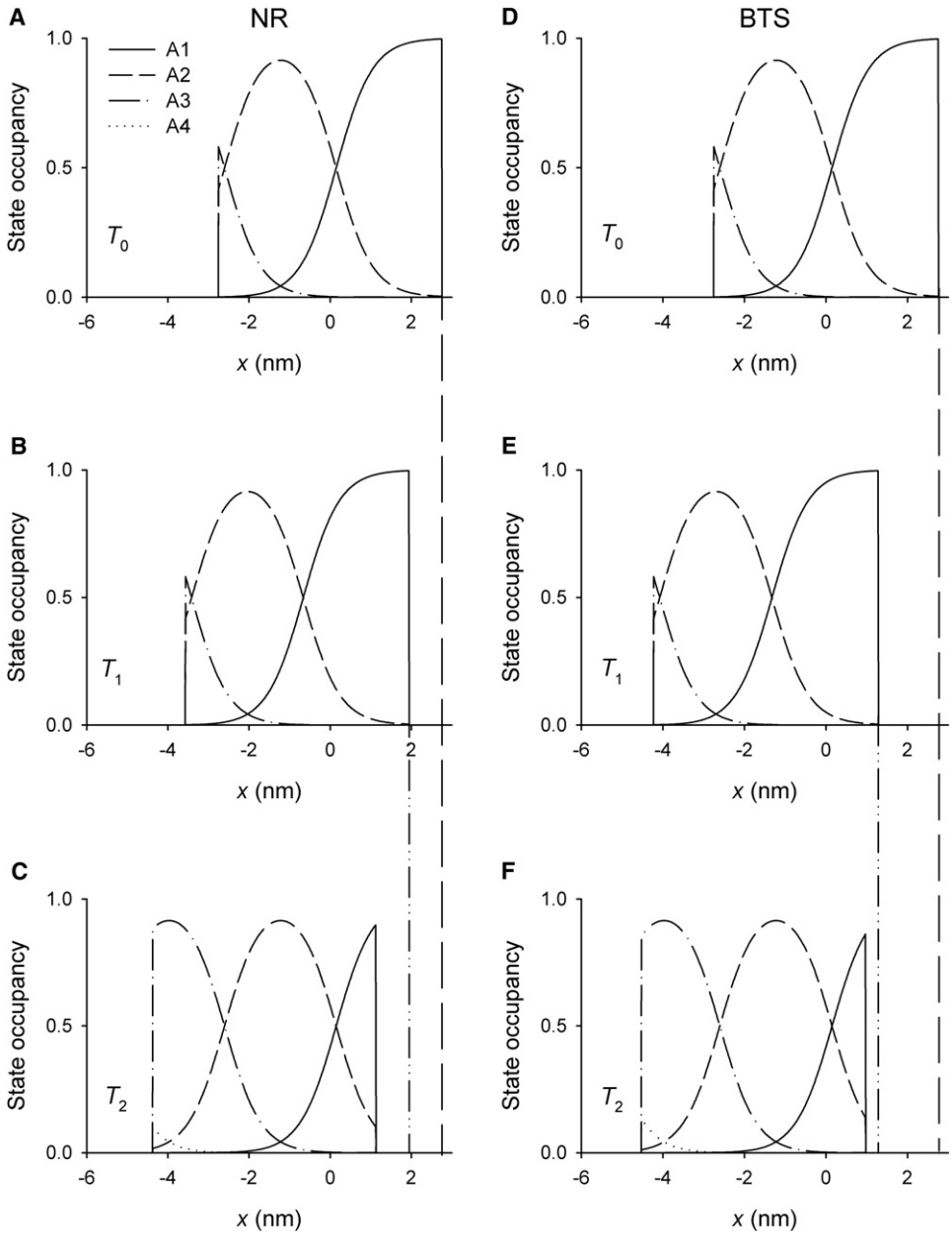

FIGURE 6 Occupancy of the various states as a function of x during the isometric contraction and at the relevant phases of the force transient elicited by a 1.85 nm step release. (*A*– *C*) control solution. (*D*–*F*) BTS solution that reduces T_0 to 0.2 $T_{0,NR}$. *A* and *D*, T_0; *B* and *E*, T_1; *C* and *F*, T_2. Solid lines *A1*, dashed lines *A2*, dotted-dashed lines *A3*, dotted lines *A4*. The vertical straight lines are the projections of the position of the rightmost position of motors at T_0 (*long dashed lines*) and at T_1 *(double dotted-dashed lines*).

was optimized for the half-sarcomere mechanical parameters of fibers from *Rana esculenta*, where, during the isometric contraction (control solution and 4 °C), the half-sarcomere strain is 3.8 nm, of which 1.7 nm (45%) are in the myosin motors (7). Consequently, the stiffness of the myosin motor (ε) is ~3 pN/nm (7, 9), more than four times larger than that assumed in the original model (0.7 pN/nm (25)) and the slope of the parabolas representing the free energy profile of attached states becomes so steep that it is impossible to fit the size and the rate of quick force recovery after length steps (28). The problem is solved if the horizontal distance between the minima of free energy parabolas is conveniently reduced and the number of parabolas is correspondingly increased to preserve a maximum working stroke of 11 nm: with a distance between minima of neighboring states, ζ, of 2.75 nm (7), the number of states must be five (*A1-A5*, Fig. 5 *A*). The difference in the minimum of free energy between neighboring states (ΔG_0) is 13 zJ and therefore the maximum mechanical energy of the working stroke is ($13 \times 5 =$) 65 zJ.

In the isometric contraction the relevant state occupancy is limited to the first two states (Figs. 5 *A* and 6 *A*), due to the high stiffness of the motor; significant occupancy of the other states occurs only when transitions through the working stroke are allowed by dropping the mechanical energy barrier represented by the isometric stress in the motor, with either a length or load release (7).

In the simulation of the quick force recovery after a step release, the reaction cycle is practically limited to the transitions between the first three force generating states of the myosin motors (Fig. 6), because the size of the length step is kept small enough to be able to assume that the force recovery is not influenced by detachment/attachment of motors. Moreover, given the recent evidence of rapid attachment of myosin motors to actin after a stretch (21), the simulation has been applied only to responses to small step releases.

In isometric contraction the motors are assumed to be distributed in the range -2.75 nm $< x < 2.75$ nm (see *thick line* in Fig. 5 *A*), where x is the reciprocal axial position between the myosin motor and the actin monomer to which it is attached and $x = 0$ when the motor in the *A1* state exerts zero force, that corresponds to the position of the free energy minimum of

the *A1* parabola. The isometric spread of motor conformations of ~5 nm is dictated not only by the constraints posed by mechanical stiffness (7,18), but also by x-ray diffraction structural studies (9,18).

The forward and reverse rate constants ($k_i(x)$ and $k_{-i}(x)$, where $i = 1, 4$) for each of the four transitions are related to the change in free energy between neighboring states ($\Delta G(x)$) through the equation:

$$\frac{k_{i(x)}}{k_{-i(x)}} = e^{\frac{\Delta G(x)}{k_b\theta}}. \quad (2)$$

The x-dependence of the rate function for the forward transition between two consecutive states is expressed according to the formalism introduced by Slawnych et al. (29) as an implementation of Huxley and Simmons formalism (5) (see Fig. 5 *B*):

$$k_{i(x)} = 30,000 \times \frac{e^{\frac{\varepsilon \times \zeta \times (x - x_{mi})}{k_b\theta}}}{1 + e^{\frac{\varepsilon \times \zeta \times (x - x_{mi})}{k_b\theta}}}. \quad (3)$$

where $\varepsilon = 3.1$ pN/nm and $\zeta = 2.75$ nm (7) and x_m is the midway position between two consecutive states. The rate function for the reverse transition is calculated from Eq. 2. For a detailed explanation of the assumptions and the definitions of parameters see Piazzesi and Lombardi (25) and Slawnych et al. (29). The distribution of attached motors in the isometric conditions, given by the sum of all state occupancy in Fig. 6, is assumed uniform in agreement with the conclusions of preceding x-ray studies (9,18), but the conclusions here are equally valid assuming a Gaussian distribution. The first step in the simulation is to select the rate equations of state transitions that best fit the time course of the quick force recovery after the step release of 1.85 nm per half-sarcomere in control solution. The algorithm for the force transient simulation in Piazzesi and Lombardi (25) is implemented to take into account that the axial position of the motors (Δz and thus x) changes with force, due to filament compliance. Filaments are under constant strain during the isometric contraction and thus, independently of the absolute value of T_0, the average axial position Δz_m of isometric motors is 0. This is expressed in the simulation by assuming that, at T_0, the axial position of motors Δz_0 ranges between $x = -2.75$ nm and $x = 2.75$ nm (see Figs. 5 *A* and 6 *A* and *D*). At T_1 after a step release of size L, Δz is given by the equation: $\Delta z_1 = \Delta z_0 + [L - C_f \times (T_1 - T_0)]$. During force recovery from T_1 to T_2, Δz is calculated at time intervals Δt of 10 μs with the equation $\Delta z_t = \Delta z_{t-\Delta t} + C_f \times (T_{t-\Delta t} - T_t)$.

The rate of quick force recovery is estimated from the simulated response with the same method used for the experimental records and plotted in Fig. 3 *B* (*rightmost solid circle*). Then the chosen set of rate equations is applied without any modification to the simulation of quick force recovery for the cases in which the myofilament compliance in series to the motors is progressively decreased in steps of 20% of the compliance in the control down to zero.

The effects of the reduction of the equivalent myofilament compliance to 20% on the axial distribution of different states of the attached motors at T_1 and T_2 after the 1.85 nm release are shown in Fig. 6. At T_1 (*B* and *E*) the state occupancy is the same as at T_0 (*A* and *B*), but shifted leftward (toward negative x) by the amount corresponding to the fraction of the release taken by the motors, Δz_1. Note that Δz_1 is quite smaller in NR than in BTS. The state transition occurs during the quick force recovery from T_1 to T_2 and is accompanied by a further shift in the axial motor distribution that is much larger in NR (*C*) than in BTS (*F*), so that at T_2 the total change in Δz is almost the same in either case (see also Fig. 4).

SUPPLEMENTARY MATERIAL

The effects of BTS on the force-velocity relation, two references, one figure, and one table are available at http://www.biophysj.org/biophysj/supplemental/S0006-3495(08)00035-0.

The authors thank Professor Malcolm Irving for helpful discussion and Mr. Mario Dolfi for technical assistance. This research was supported by the National Institutes of Health (grant R01 AR049033), by the Ministero dell'Università e della Ricerca (MIUR-COFIN 2006), and Ente Cassa di Risparmio di Firenze.

REFERENCES

1. Huxley, H. E., A. Stewart, H. Sosa, and T. Irving. 1994. X-ray diffraction measurements of the extensibility of actin and myosin filaments in contracting muscle. *Biophys. J.* 67:2411–2421.
2. Wakabayashi, K., Y. Sugimoto, H. Tanaka, Y. Ueno, Y. Takezawa, et al. 1994. X-ray diffraction evidence for the extensibility of actin and myosin filaments during muscle contraction. *Biophys. J.* 67:2422–2435.
3. Linari, M., I. Dobbie, M. Reconditi, N. Koubassova, M. Irving, et al. 1998. The stiffness of skeletal muscle in isometric contraction and rigor: the fraction of myosin heads bound to actin. *Biophys. J.* 74:2459–2473.
4. Dobbie, I., M. Linari, G. Piazzesi, M. Reconditi, N. Koubassova, et al. 1998. Elastic bending and active tilting of myosin heads during muscle contraction. *Nature.* 396:383–387.
5. Huxley, A. F., and R. M. Simmons. 1971. Proposed mechanism of force generation in striated muscle. *Nature.* 233:533–538.
6. Piazzesi, G., L. Lucii, and V. Lombardi. 2002. The size and the speed of the working stroke of muscle myosin and its dependence on the force. *J. Physiol.* 545:145–151.
7. Decostre, V., P. Bianco, V. Lombardi, and G. Piazzesi. 2005. Effect of temperature on the working stroke of muscle myosin. *Proc. Natl. Acad. Sci. USA.* 102:13927–13932.
8. Linari, M., M. Caremani, C. Piperio, P. Brandt, and V. Lombardi. 2007. Stiffness and fraction of Myosin motors responsible for active force in permeabilized muscle fibers from rabbit psoas. *Biophys. J.* 92:2476–2490.
9. Piazzesi, G., M. Reconditi, M. Linari, L. Lucii, P. Bianco, et al. 2007. Skeletal muscle performance determined by modulation of number of Myosin motors rather than motor force or stroke size. *Cell.* 131:784–795.
10. Cheung, A., J. A. Dantzig, S. Hollingworth, S. M. Baylor, Y. E. Goldman, et al. 2002. A small-molecule inhibitor of skeletal muscle myosin II. *Nat. Cell Biol.* 4:83–88.
11. Pinniger, G. J., J. D. Bruton, H. Westerblad, and K. W. Ranatunga. 2005. Effects of a myosin-II inhibitor (N-benzyl-p-toluene sulphonamide, BTS) on contractile characteristics of intact fast-twitch mammalian muscle fibres. *J. Muscle Res. Cell Motil.* 26:135–141.
12. Shaw, M. A., E. M. Ostap, and Y. E. Goldman. 2003. Mechanism of inhibition of skeletal muscle actomyosin by N-benzyl-p-toluenesulfonamide. *Biochemistry.* 42:6128–6135.
13. Huxley, A. F., and V. Lombardi. 1980. A sensitive force transducer with resonant frequency 50 kHz. *J. Physiol.* 305:15P–16P. (Abstr.)
14. Lombardi, V., and G. Piazzesi. 1990. The contractile response during steady lengthening of stimulated frog muscle fibres. *J. Physiol.* 431:141–171.
15. Huxley, A. F., V. Lombardi, and L. D. Peachey. 1981. A system for fast recording of longitudinal displacements of a striated muscle fibre. *J. Physiol.* 317:12P–13P. (Abstr.)
16. Ford, L. E., A. F. Huxley, and R. M. Simmons. 1977. Tension responses to sudden length change in stimulated frog muscle fibres near slack length. *J. Physiol.* 269:441–515.
17. Piazzesi, G., F. Francini, M. Linari, and V. Lombardi. 1992. Tension transients during steady lengthening of tetanized muscle fibres of the frog. *J. Physiol.* 445:659–711.
18. Reconditi, M., M. Linari, L. Lucii, A. Stewart, Y. B. Sun, et al. 2004. The myosin motor in muscle generates a smaller and slower working stroke at higher load. *Nature.* 428:578–581.
19. Brunello, E., P. Bianco, G. Piazzesi, M. Linari, M. Reconditi, et al. 2006. Structural changes in the myosin filament and cross-bridges during active force development in single intact frog muscle fibres: stiffness and X-ray diffraction measurements. *J. Physiol.* 577:971–984.

20. Piazzesi, G., M. Reconditi, M. Linari, L. Lucii, Y. B. Sun, et al. 2002. Mechanism of force generation by myosin heads in skeletal muscle. *Nature*. 415:659–662.

21. Brunello, E., M. Reconditi, R. Elangovan, M. Linari, Y. B. Sun, et al. 2007. Skeletal muscle resists stretch by rapid binding of the second motor domain of myosin to actin. *Proc. Natl. Acad. Sci. USA*. 104:20114–20119.

22. Straight, A. F., A. Cheung, J. Limouze, I. Chen, N. J. Westwood, et al. 2003. Dissecting temporal and spatial control of cytokinesis with a myosin II Inhibitor. *Science*. 299:1743–1747.

23. Kovacs, M., J. Toth, C. Hetenyi, A. Malnasi-Csizmadia, and J. R. Sellers. 2004. Mechanism of blebbistatin inhibition of myosin II. *J. Biol. Chem.* 279:35557–35563.

24. Allingham, J. S., R. Smith, and I. Rayment. 2005. The structural basis of blebbistatin inhibition and specificity for myosin II. *Nat. Struct. Mol. Biol.* 12:378–379.

25. Piazzesi, G., and V. Lombardi. 1995. A cross-bridge model that is able to explain mechanical and energetic properties of shortening muscle. *Biophys. J.* 68:1966–1979.

26. Colomo, F., V. Lombardi, and G. Piazzesi. 1989. The recovery of tension in transients during steady lengthening of frog muscle fibres. *Pflugers Arch.* 414:245–247.

27. Piazzesi, G., M. Linari, and V. Lombardi. 1994. The effect of hypertonicity on force generation in tetanized single fibres from frog skeletal muscle. *J. Physiol.* 476:531–546.

28. Huxley, A. F., and S. Tideswell. 1996. Filament compliance and tension transients in muscle. *J. Muscle Res. Cell Motil.* 17:507–511.

29. Slawnych, M. P., C. Y. Seow, A. F. Huxley, and L. E. Ford. 1994. A program for developing a comprehensive mathematical description of the crossbridge cycle of muscle. *Biophys. J.* 67: 1669–1677.